0026-895X/93/051046-05$03.00/0

MOLECULAR PHARMACOLOGY, 44:1046-1050

Pharmacological Characterization of α-Bungarotoxin-Sensitive Acetylcholine Receptors Immunoisolated from Chick Retina: Contrasting Properties of α7 and α8 Subunit-Containing Subtypes

RENÉ ANAND, XIAO PENG, JUAN J. BALLESTA, and JON LINDSTROM

Department of Neuroscience, University of Pennsylvania, Philadelphia, Pennsylvania 19104-6074

Received April 7, 1993; Accepted August 2, 1993

SUMMARY

At least three subtypes of α-bungarotoxin-sensitive acetylcholine receptors (αBgt-sensitive AChRs) exist in chick brain and retina. All may contain previously unknown structural subunits. One subtype contains α7 subunits. Another contains α8 subunits. A third contains both α7 and α8 subunits. In this article, we describe, for the first time, the pharmacological characterization of α7 AChRs and α8 AChRs immunoisolated from chick retina. Pharmacologically, the α8 AChRs exhibit two classes of binding sites, the high affinity of which have higher affinity for most cholinergic ligands than do α7 AChRs. These differences are most accentuated for ACh (~5400-fold), decamethonium (~1400-fold), 1,1,-dimethyl-4 phenylpiperazinium (~200-fold), atropine (~200-fold), nicotine (~100-fold), and tetramethylammonium (~100-fold). The α8 AChR low affinity sites exhibit affinities that are similar but not identical to that of α7 AChRs. Many of the pharmacological differences between the α7 AChRs and α8 AChRs can be attributed to the limited differences between the amino acid sequences of the N-terminal region of the α7 and α8 subunits because expressed α7 homomers and α8 homomers also exhibit these characteristic differences.[1]

The well-characterized αBgt-sensitive muscle-type AChR from Torpedo electric organ has provided the foundation for understanding the structure and function of all the neuronal AChRs and other members of the ligand-gated ion channel superfamily (reviewed in Refs. 1-3). αBgt-binding sites with nicotinic binding character also have been known to exist in the central and peripheral nervous system (reviewed in Refs. 4 and 5). However, most of the neuronal AChRs whose subunit cDNAs were cloned initially appeared not to be sensitive to αBgt when expressed as functional AChRs in oocytes (reviewed in Ref. 6) and mAbs to AChR α1, α3, α4, α5, β1, β2, β4, γ, or δ subunits do not immunoprecipitate neuronal AChRs that bind αBgt (7-11).

The cloning of two subunits of the αBgt-sensitive AChRs, α7 and α8 (12, 13), has elicited new interest in characterizing these elusive AChRs. A recent wave of articles triggered by the cloning of the α7 cDNA describe and dissect the functional properties of α7 homomers such as desensitization (14), affinity for cholinergic ligands (15-18), and ion selectivity (19).

Characterization of the native αBgt-sensitive AChRs, however, is still in its infancy (reviewed in Ref. 5). Immunoaffinity purification of αBgt-sensitive AChRs from chick brain and retina reveals the existence of at least three subtypes: an α7-containing subtype (termed α7 AChR), which predominates in brain; an α8-containing subtype (termed α8 AChR), which predominates in retina; and a third subtype containing both α7 and α8 subunits (termed α7α8 AChR), which is not as abundant either in brain or retina (13, 20-22). Affinity-purified αBgt-sensitive AChRs appear to be composed of more than a single type of subunit. Preparations not fractionated into α7 and α8 AChR subtypes are reported to consist of at least three different protein bands of apparent molecular masses of ~52 kDa, ~57 kDa, and ~67 kDa (23). However, the complete subunit composition of no subtype has been determined. The ~57 kDa band has been reported to correspond to the α7 subunit (24). Limited functional characterization of these AChRs, using electrophysiological methods (25, 26) and calcium-imaging techniques (27), have been carried out. Previously, we showed that α7 AChRs have the high affinity for αBgt expected of such AChRs (K_d =

This work is supported by grants from the National Institutes of Health (NS11323), the Muscular Dystrophy Association, the National Science Foundation (BNS 91-96053), the Council for Tobacco Research, USA, Inc., and the Smokeless Tobacco Research Council, Inc. R.A. is currently supported by a National Research Service Award.

ABBREVIATIONS: αBgt, α-bungarotoxin; ACh, acetylcholine; AChR, acetylcholine receptor; Deca, decamethonium; DMPP, 1,1-dimethyl-4-phenylpiperazinium; EGTA, [ethylene-bis(oxyethylenenitrilo)]tetraacetic acid; Hex, hexamethonium; mAb, monoclonal antibody; PBS, phosphate-buffered saline; RIA, radioimmunoassay; TEA, tetraethylammonium; TMA, tetramethylammonium.

2.1 nM), whereas α8 AChRs had much lower affinity for αBgt (K_d = 17.2 nM) and consequently would not have been detected by previous investigators (20).

In this article, we describe, for the first time, detailed pharmacological characterization of α7 AChRs and α8 AChRs from chick retina. We show that the α8 AChRs exhibit two classes of binding sites. The α8 AChR low affinity sites display affinities similar to those of α7 AChRs. However, the α8 AChR high affinity sites display >1000-fold higher affinity for ACh and decamethonium and >100-fold higher affinity for DMPP, atropine, nicotine, and TMA than do α7 AChRs.

Materials and Methods

Monoclonal antibodies. mAbs to α7 (318, 319) and to α8 (305, 308) have been described previously (12). Using synthetic peptides, the epitope for mAb 318 was mapped to within α7:380–400, mAb 319 to α7:365–384, and mAb 308 to α8:323–342, whereas mAb 305 binding was found to depend on the native conformation of α8 (28). The mAbs were affinity purified using protein G coupled to agarose.

Detergent solubilization of αBgt-sensitive AChRs from chick retina. Detergent extracts of αBgt-sensitive AChRs from retinae of embryonic day 18 (E18) chicks were prepared in the following manner. Retinae were dissected from the birds and then frozen at −80°. The frozen tissues were thawed in 10 vol of homogenization buffer (50 mM phosphate buffer, pH 7.5, 1 M NaCl, 5 mM EDTA, 5 mM EGTA, 2 mM phenylmethylsulfonyl fluoride, 5 mM benzamidine, 5 mM iodoacetamide) and then homogenized on ice for 2 min at 15,000 rpm with a Brinkman Polytron. After dilution with another 10 vol of the homogenization buffer, the homogenate was centrifuged at 50,000 rpm in a Beckman 50.2 Ti rotor for 30 min at 4°. The pellet was homogenized again in an equal volume of buffer, this time containing only 50 mM NaCl, and centrifuged to further extract-soluble components. The pellet was then extracted with 4 vol of a solubilization buffer (2% Triton X-100, 50 mM NaCl, 50 mM sodium phosphate, pH 7.5), and the same mix of chelating agents and protease inhibitors was used in the homogenization buffer. After initial disruption of the pellet for 15 sec at 10,000 rpm with a Brinkman Polytron, the resuspended pellet was shaken for 2 hr at 4°. The mix was then centrifuged at 50,000 rpm in a Beckman 50.2 Ti rotor at 4° for 30 min and the clear supernatant was used for subsequent experimentation. The concentration of αBgt-sensitive AChRs in the resulting extracts was typically 1–2 nM.

Immunoaffinity separation of α7 AChRs and α8 AChRs. Detergent extracts of E18 retina were depleted of all α8-containing AChRs (i.e., α8 AChRs and α7α8 AChRs) using purified mAb 305 coupled at 2 mg/ml of gel to Actigel ALD (Sterogene) according to the manufacturer's instructions. Extracts were incubated at 4° using gentle agitation with mAb 305-coupled beads at a ratio of 1:7 (bead/extract) overnight. The beads were then removed by brief centrifugation. The efficacy of depletion was then tested by solid phase RIAs using mAb 305-coated microwells and 100 nM ^{125}IαBgt. Similarly, retina extracts were depleted of all α7-containing AChRs (i.e., α7 AChRs and α7α8 AChRs) using purified mAb 318 coupled at 5 mg/ml of gel to AffiGel H2 (BioRad) according to the manufacturer's directions. The mAb 318-coupled beads were then used in depletion experiments in the same way as were the mAb 305-coupled beads. The extent of depletion of α7-containing AChRs was determined by solid phase RIAs using mAb 318-coated microwells and 50 nM ^{125}IαBgt. Bound ^{125}IαBgt was determined by gamma counting. Nonspecific binding was determined using microwells not coated with mAbs.

Radioimmunoassays. The total amount of αBgt-sensitive AChRs and the efficacies of depletion of the subtypes were determined by solid phase RIAs using mAb-coated microwells. Protein G affinity column-purified mAb 305 and 318 were coupled to Immulon 4 Removawells (Dynatech) by incubating 100 μl/well of 40 μg/ml mAb in 10 mM sodium bicarbonate buffer, pH 8.8, overnight at 4°. After three washes (200 μl each) with the bicarbonate buffer, the wells were quenched with 200 μl of a solution containing 3% BSA in PBS-Tween 20 (100 mM NaCl, 10 mM sodium phosphate buffer, pH 7.5, and 0.05% Tween-20) for 2 hr. The wells were then washed three times with 200 μl of the PBS-Tween buffer.

The total amount of α7 AChRs was measured by solid phase RIAs using wells coated with mAb 318 in 100-μl assays containing 50 nM ^{125}IαBgt and the total amount of α8 AChRs was measured similarly except using mAb 305 and 100 nM ^{125}IαBgt.

Pharmacological assays. Pharmacological characterization of the chicken retina αBgt-sensitive AChRs was performed by competitive inhibition of ^{125}IαBgt binding by various ligands to immuno-immobilized AChRs on mAb-coated Immulon 4 microwells. Diluted Triton X-100 extracts (100 μl, 0.2–0.3 nM) were added to each well and incubated overnight at 4°. The wells were then washed and incubated with various concentrations of the ligands for 20 min before the addition of ^{125}IαBgt. The assays were performed in a total volume of 100 μl in duplicate and using 2 nM ^{125}IαBgt for the α7 AChRs or 20 nM ^{125}IαBgt for the α8 AChRs. After a second incubation overnight at 4°, the wells were rinsed three times with ~200 μl of PBS-Tween 20 buffer and then counted in a gamma counter.

Data analysis. Experimental data from the α7 AChRs fitted well to the Hill equation. Experimental data for the α8 AChRs were fitted to one- and two-binding site models using a nonlinear least square analysis program, and F tests (29) were performed to test whether the fits were significantly better to the one- or two-binding site model.

Results

Immunoaffinity separation of α7 AChR and α8 AChR subtypes. We have shown previously that in E18 chick retina ~36% of all αBgt-sensitive AChRs are of the α7 AChR subtype, ~41% are of the α8 AChR subtype, and ~23% are of the α7α8 AChR subtype (20). To achieve extracts containing only α7 AChRs, we depleted Triton X-100 extracts of retina with mAb 305-coupled agarose beads (anti-α8 mAb beads) and tested the efficacy of depletion by solid phase RIAs using mAb 305-coated microwells. In this way, we typically achieved >99% depletion of all α8-containing AChRs (i.e., both the α8 AChRs and the α7α8 AChRs). Using a similar strategy, Triton X-100 extracts of retina were depleted of all α7-containing AChRs (i.e., both the α7 AChRs and α7α8 AChRs) using mAb 318-coupled agarose beads (anti-α7 mAb beads) and the efficacy of depletion was tested by solid phase RIAs using mAb 305-coated microwells. Unlike the depletion of the α8-containing AChRs, depletion of all α7-containing AChRs ranged between 90–95%, despite two successive cycles of depletion using large excesses of mAb-coupled agarose beads, probably because of the lower affinity of mAb 318 for α7 AChRs. Depleted extracts were then used for all pharmacological assays.

Pharmacological characterization of the α7 AChRs. Pharmacological characterization to test the relative efficacies by which various ligands inhibit binding of ^{125}IαBgt to the α7 AChRs was carried out by solid phase RIAs using various concentrations of ligands. Competitive inhibition of ^{125}IαBgt binding was carried out in the presence of 2 nM ^{125}IαBgt, which is close to its K_d = 2.1 nM (20). Fig. 1 (top) shows the ^{125}IαBgt inhibition curves for typical cholinergic agonists and Fig. 2 (top) for typical cholinergic antagonists and also for an atypical ligand, strychnine. The relative efficacies of the ligands were found to be: αBgt >> nicotine ≈ cytisine > curare ≈ strychnine > trimethaphan > DMPP ≈ atropine ≈ ACh > TMA ≈ Deca > TEA > carbamylcholine ≈ Hex. The affinities of the various ligands did not appear to be influenced by the binding of mAb 318 to the solubilized AChR, because nearly identical affinities

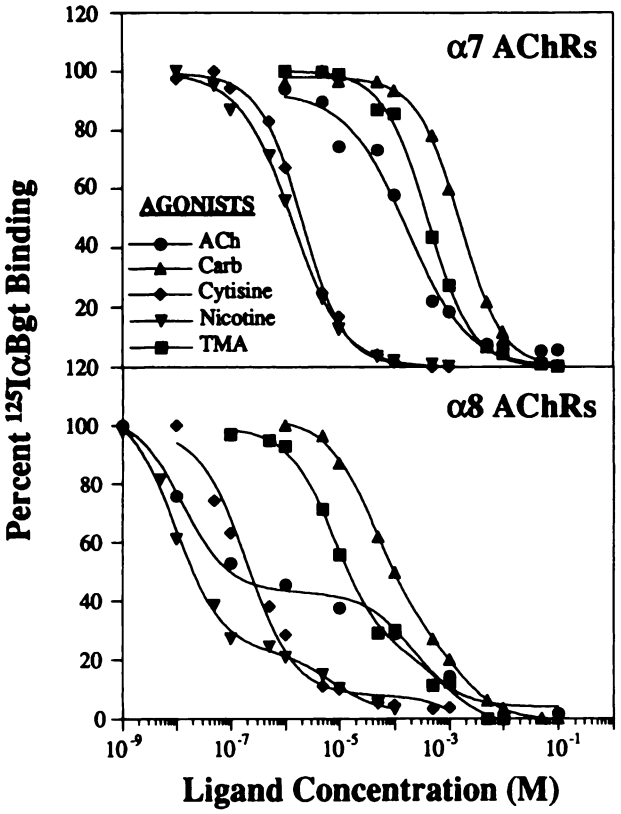

Fig. 1. Agonist Profiles of Detergent-Solubilized $\alpha 7$ AChRs and $\alpha 8$ AChRs. Pharmacological characterization was performed by competitive inhibition of ^{125}IαBgt binding by various ligands to AChRs solubilized with Triton X-100 and then immuno-immobilized on Immulon 4 microwells coated with either antibody specific for $\alpha 7$ subunits (mAb 318) or antibody specific for $\alpha 8$ subunits (mAb 305). Competitive inhibition was performed in the presence of either 2 nM (for $\alpha 7$ AChRs) or 20 nM (for $\alpha 8$ AChRs) ^{125}IαBgt. Representative dose-response curves from one experiment are shown. The curves are the best fits obtained with the Hill equation (for the $\alpha 7$ AChRs), and a two site equation (for the $\alpha 8$ AChRs). Each data point is the mean of the values obtained from duplicate determinations. The figure shows competitive inhibition of ^{125}IαBgt binding by the agonists ACh, Carb, cytisine, nicotine and TMA to $\alpha 7$ AChRs (top panel) and to $\alpha 8$ AChRs (bottom panel).

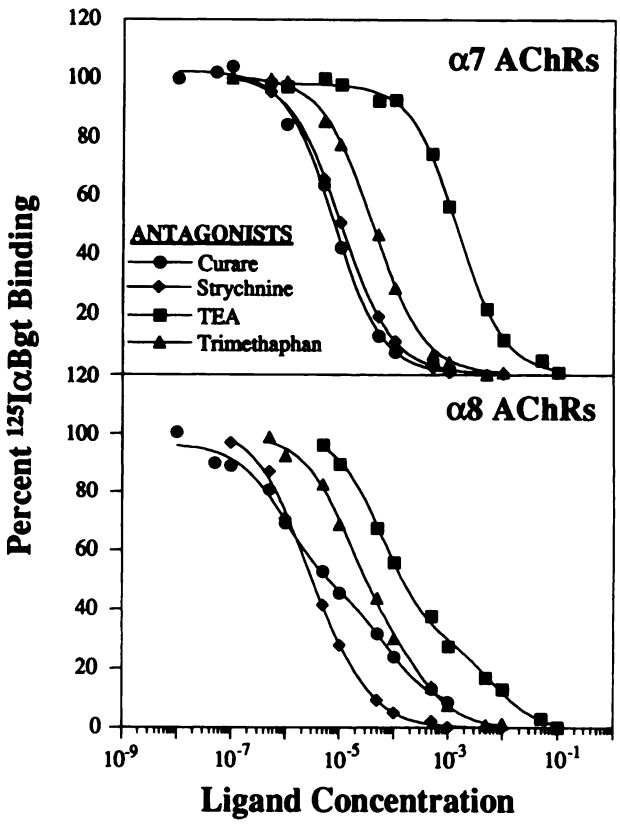

Fig. 2. Antagonist Profiles of Detergent-Solubilized $\alpha 7$ AChRs and $\alpha 8$ AChRs. Pharmacological characterization was performed by competitive inhibition of ^{125}IαBgt binding by various ligands to AChRs solubilized with Triton X-100 and then immuno-immobilized on Immulon 4 microwells coated with either antibody specific for $\alpha 7$ subunits (mAb 318) or antibody specific for $\alpha 8$ subunits (mAb 305). Competitive inhibition was performed in the presence of either 2 nM (for $\alpha 7$ AChRs) or 20 nM (for $\alpha 8$ AChRs) ^{125}IαBgt. Representative dose-response curves from one experiment are shown. The curves are the best fits obtained with the Hill equation (for the $\alpha 7$ AChRs), and a two site equation (for the $\alpha 8$ AChRs). Each data point is the mean of the values obtained from duplicate determinations. The figure shows competitive inhibition of ^{125}IαBgt binding by the antagonists curare, strychnine, TEA, and trimethaphan to $\alpha 7$ AChRs (top panel) and to $\alpha 8$ AChRs (bottom panel).

were obtained when $\alpha 7$ AChRs were tethered by mAb 319 (which maps to a nearby epitope).

Pharmacological characterization of $\alpha 8$ AChRs. The K_d of αBgt for $\alpha 8$ AChRs has been shown previously to be 17 nM (20). Hence, competitive inhibition by various ligands of ^{125}IαBgt binding to $\alpha 8$ AChR was carried out in the presence of 20 nM ^{125}IαBgt. Fig. 1 (bottom) shows the ^{125}IαBgt inhibition curves for typical agonists and Fig. 2 (bottom panel) for some antagonists. The ^{125}IαBgt inhibition curves for all ligands were better fitted for two classes of binding sites than for one class of binding sites ($p < 0.05$). The two-site fit is graphically evident for agonists ACh and nicotine (Fig. 1) and antagonist TEA and curare (Fig. 2) where the ligands exhibit large differences in affinity for the two classes of binding sites. Furthermore, this heterogeneity is not caused by the binding of mAb 305 (which binds to an epitope on the extracellular surface of the $\alpha 8$ AChR, unpublished observations) as very similar binding curves for cytisine were obtained when the solubilized $\alpha 8$ AChRs were tethered instead by mAb 308 (which maps to an intracellular epitope on the large cytoplasmic domain between transmembrane domain M3 and M4). The relative efficacies of the ligands for the high affinity site were found to be: nicotine ≈ ACh ≈ cytosine > DMPP ≈ Deca ≈ atropine ≈ curare > strychnine ≈ TMA ≈ trimethaphan > αBgt ≈ TEA ≈ carbamylcholine > Hex, whereas the relative efficacies for the low affinity site were similar to, but different from, those of $\alpha 7$ AChRs.

Table 1 summarizes the pharmacological properties of $\alpha 7$ AChRs and $\alpha 8$ AChRs. Interestingly, both subtypes display micromolar affinities for strychnine (a glycinergic antagonist) and atropine (a muscarinic antagonist). Fig. 3 demonstrates that although $\alpha 8$ AChR high affinity sites have lower affinity for αBgt than do $\alpha 7$ AChRs, $\alpha 8$ AChRs have higher affinity for all the other small ligands tested. As seen from this plot, IC_{50}s for ligands that are most displaced from the diagonal correspond to ligands that best differentiate between $\alpha 7$ AChRs and $\alpha 8$ AChR high affinity sites, i.e., ACh (~5400-fold), decamethonium (~1400-fold), DMPP (~200-fold), atropine (~200-fold), nicotine (~100-fold), and TMA (~100-fold). Some of these ligands also show characteristic differences in affinity for $\alpha 7$ homomers (17) and $\alpha 8$ homomers[1].

[1] V. Gerzanich, R. Anand, and J. Lindstrom, manuscript in preparation.

TABLE 1

Pharmacological characterization of retina α7 AChRs and α8 AChRs

The IC_{50}s shown are the mean ± SE from duplicate determinations.

Ligand	α7 AChRs (IC_{50}, μM)	α8 AChRs			
		IC_{50} (site 1), μM	Total sites (%)	IC_{50} (site 2), μM	Total sites (%)
Acetylcholine	160 ± 26	0.031 ± 0.01	55	390 ± 120	45
Atropine	120 ± 12	0.58 ± 0.12	66	53 ± 22	34
α-Bungarotoxin	0.00191 ± 0.0002[a]	0.0224 ± 0.001[a]	—	—	—
Carbamylcholine	1580 ± 320	50 ± 7	73	1400 ± 540	27
Curare	7.3 ± 2	0.79 ± 0.24	55	65 ± 28	45
Cytisine	2.0 ± 0.1	0.035 ± 0.005	67	0.94 ± 0.14	33
DMPP	83 ± 6	0.39 ± 0.09	71	26 ± 15	29
Decamethonium	680 ± 21	0.47 ± 0.17	45	2800 ± 1900	55
Hexamethonium	1650 ± 510	190 ± 53	59	6200 ± 2300	41
L-nicotine	1.3 ± 0.6	0.012 ± 0.002	78	11 ± 5	22
Strychnine	9.9 ± 0.4	2.0 ± 0.4	76	18 ± 12	24
Tetraethylammonium	1420 ± 3	57 ± 9	70	5700 ± 1500	30
Tetramethylammonium	400 ± 110	8.0 ± 1	77	700 ± 360	23
Trimethaphan	38.0 ± 7	13 ± 3	66	240 ± 100	34

[a] K_D.

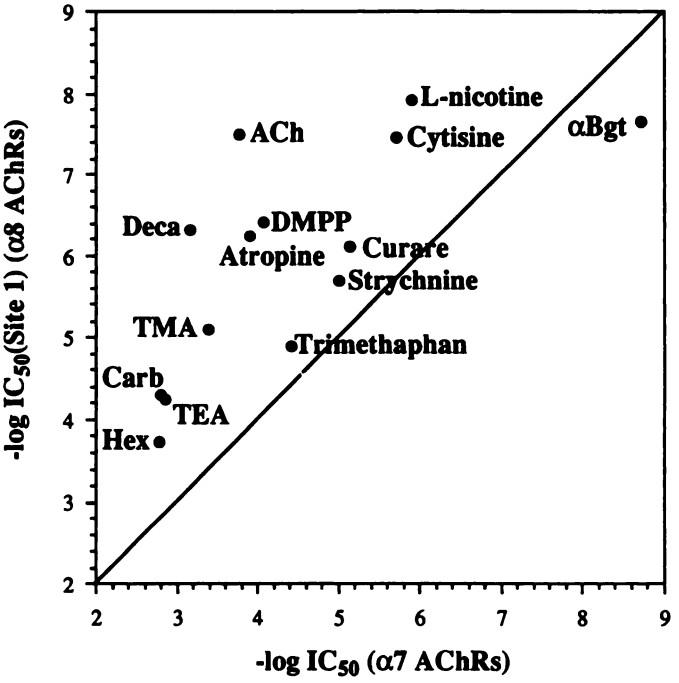

Fig. 3. Correlation of Affinities for Various Ligands Between α7 AChRs and α8 AChRs. A comparison of the affinities of detergent solubilized α7 AChRs and α8 AChR high affinity site is shown as a log IC_{50}-log IC_{50} plot. The diagonal line shows the expected result if α7 AChRs and α8 AChRs had identical affinities. Points displaced to the left indicate higher affinity for α8 AChRs - in fact, this includes all small cholinergic ligands tested. Points displaced to the right indicate higher affinity for α7 AChRs - in fact this applied only to αBgt among the ligands tested.

Discussion

Native αBgt-sensitive AChRs from brain and retina have not yet been fully characterized. Their subunit composition and stoichiometry have yet to be elucidated and none of the other cloned neuronal AChR subunits is thought to be associated with the α7 and α8 subunits in their native state. However, cloning of the α7 and α8 subunit cDNAs, and the subsequent use of their cytoplasmic domain fragments as immunogens, has allowed us to raise subunit-specific mAbs (12). These mAbs have been used to histologically localize α7 AChRs, α8 AChRs, and α7α8 AChRs in both chick brain and retina (20–22, 30) and α7 AChRs in rat brain.[2] Using these α7 and α8 subunit-specific mAbs and Triton X-100 extracts of chick retina, we have immunoisolated α7 AChR subtypes from α8 AChR subtypes. Scatchard analysis of ^{125}IαBgt binding to these two subtypes had previously indicated that α7 AChRs exhibited ~10-fold higher affinity for αBgt than did α8 AChRs (20).

In this article, we describe a more complete pharmacological characterization of the α7 and α8 AChRs. Using competitive inhibition of ^{125}IαBgt binding by various ligands to α7 AChRs and α8 AChRs, we show that the α8 AChRs show further heterogeneity in that they exhibit two classes of binding sites. The α8 AChR high affinity sites show between 100–1000-fold higher affinity for ACh, Deca, DMPP, atropine, nicotine, and TMA than do α7 AChRs, whereas the α8 AChR low affinity sites exhibit affinities of the same order, but distinct from, α7 AChRs.

The simplest explanations for the two classes of binding sites in α8 AChRs are: 1) intramolecular heterogeneity and 2) intermolecular heterogeneity. The intramolecular heterogeneity could be generated by association of α8 subunits with different structural subunits as would be in an AChR of subunit composition α8βxα8βyβz or by heterogeneity in the α-subunit as would be in an AChR of subunit composition α8βxαyβxβx. There is a precedent for the former case in muscle-type α1γα1δβ AChRs, where the two binding sites are formed at the α1- and γ-interface and the α1- and δ-interface (31). However, an alternative possibility is that the two sites are the result of two subtypes of α8 AChRs, wherein each subtype is generated by association of the α8 subunit with different structural subunits as would be in a mix of AChRs of composition α8βxα8βxβx and α8βyα8βyβy.

Pharmacological characterization of α7 homomers (13, 17, 18) and α8 homomers[1] expressed in oocytes reveals that α8 homomers also display striking differences in their affinity for ACh, cytosine, and DMPP, when compared with α7 homomers. Thus, it appears that the pharmacological differences observed between the native α7 AChRs and the native α8 AChRs may be accounted for, to some degree, by the differences between the amino acid sequences of α7 and α8 subunits. However, while detergent-solubilized native α7 AChRs do not appear to show marked a difference in their affinity for most cholinergic ligands when compared with detergent-solubilized α7 homomers expressed in oocytes (18), they do show a ~50-fold differ-

[2] P. Juiz, M. Criado, and J. Lindstrom, unpublished observations.

ence in their affinity for cytosine, which we take to be indicative of the presence of structural subunits in the native αBgt-sensitive AChRs. It has been shown previously that cytosine, a rigid ACh analogue, is very sensitive to the presence of structural subunits because α3β2 AChRs show ~100-fold difference in affinity for cytosine when compared with α3β4 AChRs (32). Thus, structural subunits do appear to participate in binding to or indirectly influence the binding of α7 AChRs and α8 AChRs to at least some of the ligands.

In summary, we have demonstrated a paradoxical difference in pharmacological properties of α7 AChRs and α8 AChR high affinity sites: Although α8 AChR high affinity sites have lower affinity for αBgt than do α7 AChRs (and consequently have evaded detection by previous investigators who have labeled tissue with <5 nM αBgt), nonetheless, α8 AChR high affinity sites have much higher affinity for all small cholinergic ligands tested. Because it turns out that these pharmacological properties are also true of α7 homomers (18) and α8 homomers,[1] future *in vitro* mutagenesis experiments with these homomers that take advantage of the limited sequence differences between α7 and α8 subunits may be able to define many of the amino acids responsible for the differences in pharmacological properties between α7 AChRs and α8 AChR high affinity sites. The relatively high affinity of α8 AChRs for small cholinergic ligands suggests that these AChRs may play a larger role in the effects of nicotine and other cholinergic ligands *in vivo* than might previously have been expected of neuronal AChRs that bind αBgt. Another interesting anomaly is the relatively high affinity of α8 AChRs for the muscarinic antagonist atropine or the glycinergic antagonist strychnine. For example, atropine has slightly higher affinity than the classic nicotinic antagonist curare, and strychnine has less than 3-fold lower affinity than curare.

Future experiments will also be necessary to purify and analyze the complete subunit compositions and stoichiometries of the αBgt AChR subtypes. Then it will be necessary to test this analysis by co-expressing these combinations of subunits from their cDNAs and determining whether the expressed AChRs exhibit pharmacological properties identical to those of native AChRs described here.

Acknowledgments

We thank John Cooper for iodinations, Lorie Criswell for mAb purifications, Chien-Yean Cheng, Shin Young Jun, Michael Katz, Trilby Tener, and Dore Wong for technical assistance, Dawn McCullough for preparation of the manuscript, and Mike White (Medical College of Pennsylvania) and all the other members of the laboratory for comments on the manuscript.

References

1. Changeux, J.-P. Functional architecture and dynamics of the nicotinic acetylcholine receptor: an allosteric ligand-gated ion channel, in *Fidia Research Foundation Neuroscience Award Lectures (J. P. Changeux, R. R. Llinas, D. Purves, and F. E. Bloom, eds.).* Vol. 4, p. 21–168, Raven Press, New York (1990).
2. Karlin, A. Exploration of the nicotinic acetylcholine receptor. *Harvey Lect.* **85**:71–107 (1991).
3. Unwin, N. Neurotransmitter action: opening of ligand-gated ion channels. *Neuron* **10**:31–41 (1993).
4. Schmidt, J. Biochemistry of nicotinic acetylcholine receptors in the vertebrate brain. *Int. Rev. Neurobiol.* **30**:1–38 (1988).
5. Clarke, P. B. S. The fall and rise of neuronal α-bungarotoxin binding proteins. *Trends Pharmacol. Sci.* **13**:407–413 (1992).
6. Deneris, E. S., J. Connolly, S. W. Rogers, and R. Duvoisin. Pharmacological and functional diversity of neuronal nicotinic acetylcholine receptors. *Trends Pharmacol. Sci.* **12**:34–40 (1991).
7. Whiting, P., and J. Lindstrom. Characterization of bovine and human neuronal nicotinic receptors using monoclonal antibodies. *J. Neurosci.* **8**:3395–3404 (1988).
8. Whiting, P., J. Cooper, J. Lindstrom. Antibodies in sera from patients with myasthenia gravis do not bind to nicotinic receptors from human brain. *J. Neuroimmunol.* **16**:205–213 (1987).
9. Schoepfer, R., S. Halvorsen, W. Conroy, P. Whiting, and J. Lindstrom. Antisera against an α3 fusion protein bind to ganglionic but not brain nicotinic acetylcholine receptors. *FEBS Lett.* **257**:393–399 (1989).
10. Conroy, W., A. Vernallis, and B. Berg. The α5 gene product assembles with multiple acetylcholine receptor subunits to form distinctive receptor subtypes in brain. *Neuron* **9**:1–20 (1992).
11. Vernallis, A., B. Conroy, and D. Berg. Neurons assemble acetylcholine receptors with as many as three kinds of subunits while maintaining segregation among receptor subtypes. *Neuron* **10**:451–464 (1993).
12. Schoepfer, R., W. G. Conroy, P. Whiting, M. Gore, and J. Lindstrom. Brain α-bungarotoxin binding protein cDNAs and mAbs reveal subtypes of this branch of the ligand-gated ion channel gene family. *Neuron* **5**:35–48 (1990).
13. Couturier, S., D. Bertrand, J.-M. Matter, M.-C. Hernandez, S. Bertrand, N. Millar, S. Valera, T. Barkas, and M. Ballivet. A neuronal nicotinic acetylcholine receptor subunit (α7) is developmentally regulated and forms a homooligomeric channel blocked by α-Btx. *Neuron* **5**:847–856 (1990).
14. Revah, F., D. Bertrand, J.-L. Galzi, A. Devillers-Thiery, C. Mulle, N. Hussy, S. Bertrand, M. Ballivet, and J.-P. Changeux. Mutations in the channel domain alter desensitization of a neuronal nicotinic receptor. *Nature* **353**:846–849 (1991).
15. Galzi, J.-L., D. Bertrand, A. Devillers-Thiéry, F. Revah, S. Bertrand, and J.-P. Changeux. Functional significance of aromatic amino acids from three peptide loops of the α7 neuronal nicotinic receptor site investigated by site-directed mutagenesis. *FEBS Lett.* **294**:198–202 (1991).
16. Bertrand, D., A. Devillers-Thiery, F. Revah, J.-L. Galzi, N. Hussy, C. Mulle, S. Bertrand, M. Ballivet, and J.-P. Changeux. Unconventional pharmacology of a neuronal nicotinic receptor mutated in the channel domain. *Proc. Natl. Acad. Sci. USA* **89**:1261–1265 (1992).
17. Bertrand, D., S. Bertrand, and M. Ballivet. Pharmacological properties of the homomeric α7 receptor. *Neurosci. Lett.* **146**:87–90 (1992).
18. Anand, R., X. Peng, and J. Lindstrom. Homomeric and native α7 acetylcholine receptors exhibit remarkably similar but nonidentical pharmacological properties suggesting that the native receptor is a heteromeric protein complex. *FEBS Lett.* **327**:241–246 (1993).
19. Sèguèla, P., J. Wadiche, K. Dineley-Miller, J. A. Dani, and J. W. Patrick. Molecular cloning, functional properties, and distribution of rat brain α7: a nicotinic cation channel highly permeable to calcium. *J. Neurosci.* **13**:596–604 (1993).
20. Keyser, K. T., L. R. G. Britto, R. Schoepfer, P. Whiting, J. Cooper, W. Conroy, A. Brozozowska-Prechtl, J. H. Karten, and J. Lindstrom. Three subtypes of α-bungarotoxin-sensitive nicotinic acetylcholine receptors are expressed in chick retina. *J. Neurosci.* **13**:442–454 (1993).
21. Britto, L. R. G., K. T. Keyser, J. M. Lindstrom, and H. J. Karten. Immunohistochemical localization of nicotinic acetylcholine receptor subunits in the mesencephalon and diencephalon of the chick (*Gallus gallus*). *J. Comp. Neurol.* **317**:325–340 (1992).
22. Britto, L. R. G., D. E. Hamassaki-Britto, E. S. Ferro, K. T. Keyser, H. J. Karten, and J. M. Lindstrom. Neurons of the chick brain and retina expressing both α-bungarotoxin-sensitive and α-bungarotoxin-insensitive nicotinic acetylcholine receptors: an immunohistochemical analysis. *Brain Res.* **590**:193–200 (1992).
23. Gotti, C., A. E. Ogando, W. Hanke, R. Schlue, M. Moretti, and F. Clementi. Purification and characterization of an α-bungarotoxin receptor that forms a functional nicotinic channel. *Proc. Natl. Acad. Sci. USA* **88**:3258–3262 (1991).
24. Gotti, C., W. Hanke, W.-R. Schlue, L. Briscini, M. Morett, and F. Clementi. A functional α-bungarotoxin receptor is present in chick cerebellum: purification and characterization. *Neuroscience* **50**:117–127 (1992).
25. Alkondon, M., and E. X. Albuquerque. Initial characterization of the nicotinic acetylcholine receptors in rat hippocampal neurons. *J. Recept. Res.* **11**:1001–1022 (1991).
26. Zorumski, C. F., L. L. Thio, K. E. Isenberg, and D. B. Clifford. Nicotinic acetylcholine currents in cultured postnatal rat hippocampal neurons. *Mol. Pharmacol.* **41**:931–936 (1992).
27. Vijayaraghavan, S., P. C. Pugh, Z-W. Zhang, M. M. Rathouz, and D. K. Berg. Nicotinic receptors that bind α-bungarotoxin on neurons raise intracellular free Ca^{++}. *Neuron* **8**:353–362 (1992).
28. McLane, K. E., X. Wu, J. M. Lindstrom, and B. M. Conti-Tronconi. Epitope mapping of polyclonal and monoclonal antibodies against two α-bungarotoxin binding α subunits from neuronal nicotinic receptors. *Neuroimmunology* **38**:115–128 (1992).
29. Munson, P. J., and D. Rodbard. LIGAND: a versatile computerized approach for characterization of ligand-binding systems. *Anal. Biochem.* **107**:220–239 (1980).
30. Hamassaki-Britto, D. E., A. Brozozowska-Prechtl, H. Karten, and J. Lindstrom. Bipolar cells of the chick retina containing α bungarotoxin-sensitive nicotinic acetylcholine receptors. *Visual Neurosci.*, in press.
31. Blount, P., and J. P. Merlie, Molecular basis of the two nonequivalent ligand binding sites of the muscle nicotinic acetylcholine receptor. *Neuron* **3**:349–357 (1989).
32. Luetje, C. W., and J. Patrick. Both α- and β-subunits contribute to the agonist sensitivity of neuronal nicotinic acetylcholine receptors. *J. Neurosci.* **11**:837–845 (1991).

Send reprint requests to: Jon Lindstrom, 217 Stemmler Hall, 36th and Hamilton Walk, Department of Neurological Sciences, University of Pennsylvania, Philadelphia, PA 19104–6074.